POLITECNICO DI TORINO
Repository ISTITUZIONALE

A Three-Class AI Model for Brugada Syndrome Detection to Improve Diagnostic Accuracy in ECG Analysis

Original
A Three-Class AI Model for Brugada Syndrome Detection to Improve Diagnostic Accuracy in ECG Analysis / Randazzo, V., Casella, A., Caligari, S., Gaita, F., Giustetto, C., Pasero, E.. - ELETTRONICO. - (2025). (2025 IEEE Medical Measurements & Applications (MeMeA) Chania (Gre) 28-30 May 2025) [10.1109/memea65319.2025.11067974].

Availability:
This version is available at: 11583/3002112 since: 2025-07-25T16:19:01Z

Publisher:
IEEE

Published
DOI:10.1109/memea65319.2025.11067974

Terms of use:

This article is made available under terms and conditions as specified in the corresponding bibliographic description in the repository

Publisher copyright
IEEE postprint/Author's Accepted Manuscript

©2025 IEEE. Personal use of this material is permitted. Permission from IEEE must be obtained for all other uses, in any current or future media, including reprinting/republishing this material for advertising or promotional purposes, creating new collecting works, for resale or lists, or reuse of any copyrighted component of this work in other works.

(Article begins on next page)

19 November 2026

A Three-Class AI Model for Brugada Syndrome Detection to Improve Diagnostic Accuracy in ECG Analysis

Vincenzo Randazzo
DET
Politecnico di Torino
Turin, Italy
vincenzo.randazzo@polito.it

Alessandro Casella
DET
Politecnico di Torino
Turin, Italy
alessandro.casella@polito.it

Silvia Caligari
DET
Politecnico di Torino
Turin, Italy
silvia.caligari@polito.it

Fiorenzo Gaita
Department of Medical Sciences
University of Turin
J Medical
Turin, Italy

Carla Giustetto
Department of Medical Sciences
University of Turin
Città della Salute e della Scienza
Turin, Italy

Eros Pasero
DET
Politecnico di Torino
Turin, Italy
eros.pasero@polito.it

***Abstract*—Brugada Syndrome (BrS), a cardiac arrhythmia linked to sudden cardiac death (SCD), is diagnosed based on specific electrocardiographic (ECG) patterns, with Type 1 being diagnostic. Traditional binary classification models for BrS detection have struggled with diagnostic uncertainty, particularly in cases where Type 1 patterns are suggestive but not conclusive. Overlap with other ECG abnormalities, such as Right Bundle Branch Block (RBBB) and Non-Specific Intraventricular Conduction Delay (NIVCD), has further complicated classification.**

To address these challenges, a three-class system (Definitive, Borderline, non-BrS) was introduced. Initially, a binary model was adapted to ternary classification by defining probability thresholds for borderline cases, achieving approximately 85% accuracy. To fully leverage this framework, the model was modified to handle three output classes. The re-annotation process involved both the transition to a three-class system and the refinement of ground-truth labels to ensure independent classification of QRS complex and T-wave within each ECG lead.

The models were evaluated through experiments on different configurations using a hold-out validation set, with the test set kept isolated for final assessment. The best model achieved 94% accuracy, with macro-average scores of 94% precision, 93% recall, and 93% F1-score on the test set. These results demonstrate that the three-class system aligns better with clinical decision-making. This study highlights the importance of integrating clinical expertise into machine learning models for complex diagnostics.

***Index Terms*—Neural Networks, Brugada Syndrome, ECG Classification, Artificial Intelligence in Cardiology, Sudden Cardiac Death**

I. Introduction

Brugada Syndrome (BrS) is an inherited cardiac disorder characterized by specific electrocardiographic (ECG) abnormalities, first systematically described by the Brugada brothers in 1992 [1], [2]. The defining trait of BrS is the Type 1 Brugada ECG pattern, which consists of a coved-type ST-segment elevation of at least 2 mm in the right precordial leads (V1–V3), followed by a negative T wave [3]. This pattern is considered diagnostic and is associated with an increased risk of life-threatening arrhythmias, such as polymorphic ventricular tachycardia and ventricular fibrillation, which can lead to sudden cardiac death (SCD) in individuals without overt structural heart disease [1].

Advancements in Artificial Intelligence (AI) and Machine Learning (ML) have significantly improved ECG analysis for inherited arrhythmia syndromes, enabling automated pattern classification and arrhythmic risk assessment. Deep learning (DL) models have been used to predict drug-induced Brugada patterns and improve BrS diagnosis using wearable technology and ECG-based models [4]–[6]. Neural networks have shown high sensitivity in detecting patients with Short QT Syndrome [7] and have been applied to enhance BrS diagnosis and prognosis through ECG feature analysis [8]–[10]. Additionally, AI models have been developed to predict fatal arrhythmic events in BrS, further refining risk assessment [10].

Encouraged by these developments, this work focuses on automating the distinction between definite and borderline Type 1 Brugada ECG patterns using AI-based techniques. Unlike full risk stratification, which aims to predict the likelihood of life-threatening events [11], this approach is specifically designed to refine ECG-based classification by identifying cases that unequivocally meet all diagnostic criteria versus those that do not fully satisfy them.

Unlike traditional binary approaches, this three-way classification identifies a borderline group that may represent intermediate-risk patients. This stratification aligns with clinical practice, where ECG patterns often fall into a diagnostic gray zone requiring closer monitoring. The cases in borderline group would trigger additional tests (e.g., drug test, e.g. ajmaline [12]) rather than being dismissed as uncertain.

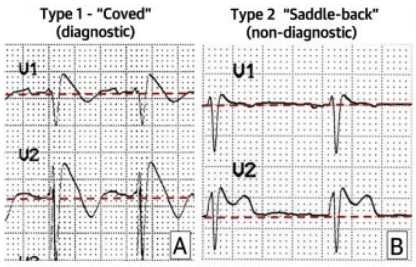


Fig. 1. Brugada syndrome ECG patterns (standard paper scale: 25 mm/s speed, 10 mm/mV amplitude).

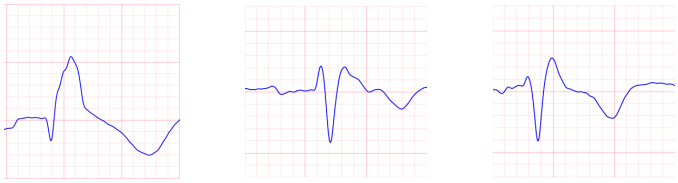


Fig. 2. ECG patterns mimicking Brugada syndrome type 1 (standard paper scale: 25 mm/s speed, 10 mm/mV amplitude): (left) complete right bundle branch block (RBBB), (center) incomplete RBBB, and (right) nonspecific intraventricular conduction delay (NIVCD).

The novelty of the work does not lie in the model architecture itself, but rather in the redefinition of the BrS classification problem to explicitly handle doubtful ECG patterns as a third class.

This paper is structured as follows: Section II provides background information on BrS and discusses the clinical relevance of its ECG patterns. Section III presents the methodology, including dataset characteristics, feature extraction techniques, and model architecture. Section IV reports the experimental findings, comparing classification performances across different models and discussing their implications for clinical practice. Finally, Section V summarizes the key contributions and outlines potential future developments in AI-assisted BrS detection.

II. Background

Brugada Type 1 pattern is considered diagnostic, while the Type 2 pattern presents a saddle-back morphology, which may require further clinical assessment to confirm BrS (Fig. 1). However, these ECG patterns can be intermittent or influenced by external factors, leading to diagnostic uncertainty. Recent studies highlight progress in both diagnosis and management of the syndrome [13], [14].

For these reasons, diagnosing Type 1 BrS can be challenging, especially in cases where the ECG does not fully meet all three diagnostic criteria in one of the right precordial leads: (i) coved-type ST-segment elevation, (ii) J-point elevation $\geq 2\,mm$ (i.e., ≥ 0.2 mV), and (iii) a negative T wave [3]. When one of these criteria is not entirely met, the classification of the ECG becomes uncertain (Borderline), adding complexity to clinical decision-making and patient management.

An additional challenge is distinguishing Brugada patterns from other conditions with similar ST-segment elevations, such as right bundle branch block (RBBB) and nonspecific intraventricular conduction delay (NIVCD). Figure 2 (each small square on the ECG paper corresponds to 1 mm in length) illustrates these similarities, emphasizing the need for advanced computational tools to improve discrimination [15], [16].

III. Methods

A. Preliminary Analysis and Motivation behind the Study

This analysis builds upon a pre-existing binary classification model designed by Caligari et al. [17] to distinguish Brugada from non-Brugada QRS complexes with T-wave. This model demonstrated high performance, achieving an accuracy of 0.96 on its dedicated test set, with a sensitivity (recall) of 0.90. However, in clinical practice, variability in expert interpretations often leads to discrepancies in the classification of borderline cases, where Brugada patterns are not clearly distinguishable and can be easily mistaken for other conduction abnormalities, such as RBBB and NIVCD. To account for this diagnostic uncertainty, a third, intermediate class was introduced to better capture ambiguous cases, providing a more refined classification framework.

As a preliminary approach to extend the binary classification model to a ternary setting, it was implemented a simple post-processing strategy based on empirically defined probability thresholds to distinguish three output intervals (definitive BrS $(0.94, 1]$, borderline BrS $(0.33, 0.94]$, and non-BrS $[0, 0.33]$). The threshold intervals were chosen to maximize the accuracy on the test set, with the aim of exploring the ability of the binary model to adapt to borderline cases. Although this choice departs from standard training-validation procedures, it served an exploratory purpose and will be re-evaluated with newly collected patient data in future validations.

The original model's weights served as the starting point for fine-tuning a new three-class model, allowing the network to adapt its learned features to the expanded classification task. In addition, a from-scratch training was run to explore whether the prior non-random binary initialization might limit further improvements.

Eventually, to ensure a clinically consistent comparison with the threshold-adapted binary model, the final analysis focuses on comparing the fine-tuned three-class network and the adapted binary model, since they use the same test set. The comparison is conducted at the level of individual ECG signals from each lead, averaging the predictions across all QRST windows within the full duration of the signal, providing a perspective closer to real-world diagnosis.

B. Dataset and Preprocessing

The dataset used in this study comprises 349 12-lead ECGs collected from multiple sources. Among them, 195 ECGs were digitally recorded using the GE Healthcare MAC2000 system [18], while 154 were digitized from paper-based ECGs via PMcardio software [19] and an internal application.

TABLE I
FINAL DATASET DISTRIBUTION FOR THE FINE-TUNED MODEL (AFTER TRAINING SET DOWNSAMPLING).

Set	Non-BrS	Borderline	Definitive
Training	720	583	625
Validation	180	146	156
Test	238	172	124
Total	1138	901	953

TABLE II
FINAL DATASET DISTRIBUTION FOR THE FROM-SCRATCH MODEL (AFTER TRAINING SET OVERSAMPLING).

Set	Non-BrS	Borderline	Definitive
Training	1184	1184	1184
Validation	209	119	112
Test	240	145	133
Total	1633	1448	1429

1) Feature Extraction: For this study, 850-millisecond (ms) windows were extracted from V1, V2, and V3 leads. These windows were centered around the S peaks, identified via inverse wavelet transform [20]. Each window spanned 300 ms before and 550 ms after the S peak to ensure adequate ST-segment capture, enabling the model to focus on the most relevant portions of the ECG waveform.

2) Dataset Balancing: Due to the dataset class imbalance, specific resampling techniques were applied:

- Downsampling: Used during the fine-tuning phase, reducing the majority class (No Brugada).
- Oversampling: Applied in models trained from scratch, replicating the minority class samples.

These resampling strategies were applied exclusively to the training set; the validation and test sets were left untouched to prevent data leakage and ensure an unbiased evaluation. The original entire dataset consisted of 1633 Non-BrS, 953 Definitive, and 901 Borderline samples. The datasets used to train and test the two models were differently composed:

- Fine-tuned Model: Maintained the original train/val/test split used in pre-training the binary model to ensure data integrity.
- From-Scratch Model: Followed a 80-10-10% train/val/test split. Waveforms from each lead were confined to a single set to prevent bias, ensuring no temporally adjacent windows appeared across splits.

Tables I and II present the final class distribution after resampling for both models.

C. Neural Network Architecture

The neural network architecture was designed to process sequential ECG data with the duration of 850 ms, leveraging convolutional and recurrent layers, followed by an attention mechanism to focus on the most relevant segments of the signal. The full architecture is detailed in Table III.

The attention mechanism, adapted from [21], operates on the bidirectional LSTM outputs by learning a context vector ($u \in \mathbb{R}^{32}$) and a dense transformation matrix ($W \in \mathbb{R}^{32\times32}$). This allows the model to dynamically weigh the importance of different temporal segments without explicit query/key/value projections. The attention weights α_t for each timestep t are computed as:

$$\alpha_t = \text{softmax}(u^T \tanh(W h_t + b)) \tag{1}$$

where h_t is the LSTM output at timestep t. The final context vector is the weighted sum $\sum_t \alpha_t h_t$.

TABLE III
NEURAL NETWORK ARCHITECTURE

Layer Type	Configuration
Input Layer	Sequence length × Features
Batch Normalization	Applied multiple times throughout
Gaussian Noise	$\sigma = 0.15$
Conv1D (x2)	128 filters, kernel=3, ReLU, L2(0.02)
MaxPooling1D	pool size=2
Dropout	0.5
Conv1D (x2)	64 filters, kernel=3, ReLU, L2(0.02)
MaxPooling1D	pool size=2
Dropout	0.5
Conv1D (x2)	32 filters, kernel=3, ReLU, L2(0.02)
MaxPooling1D	pool size=2
Dropout	0.5
Bidirectional LSTM (x2)	32 units, return sequences=True
Dropout	0.5
Attention Layer	$W \in \mathbb{R}^{32\times32}$, $u \in \mathbb{R}^{32}$
Dense (x3)	32 neurons, ReLU, L2(0.02)
Dropout	0.5
Dense (Output)	3 neurons, softmax

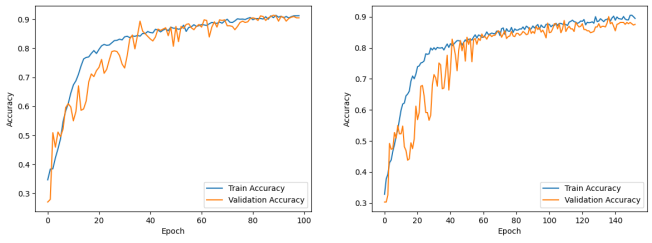
Compared to the original binary classification model, the only difference in this architecture was the output layer. Instead of a single neuron with a *sigmoid* activation function for binary classification, the final dense layer had three output neurons with a *softmax* activation function. This modification allowed the model to classify ECG patterns into three distinct categories:

- Brugada Type 1 (Definitive): ECGs that meet all clinical criteria for a definitive diagnosis, explained in Section II.
- Non-Brugada Type 1: ECGs that do not exhibit the characteristics required for a Brugada diagnosis.
- Borderline: ECGs that present some Brugada-like features but do not fully meet all the diagnostic criteria defined in Sec. II.

This adjustment required modifying the loss function as well. While the original binary model used *binary cross-entropy*, the new multi-class classification model employed *categorical cross-entropy* to appropriately handle the three-class prediction task. The rest of the architecture, including convolutional feature extraction, recurrent temporal analysis, and attention mechanisms, remained unchanged.

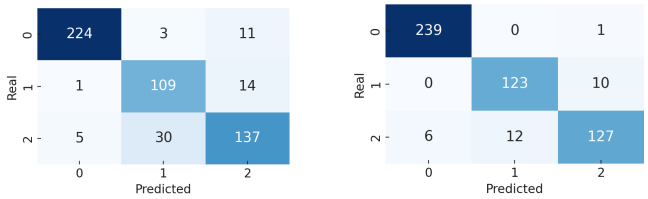
D. Training Progress Comparison

The trend of the training curves reveals fundamentally different learning behaviours between the two approaches.



(a) Model trained from-scratch (b) Fine-tuned model

Fig. 3. Training and validation accuracy trends.



(a) Fine-tuned model (b) Model trained from scratch

Fig. 4. Confusion matrices of the two models on the tests set (Class 0 is Non-Brs, Class 1 is Definitive, Class 2 is Borderline).

The from-scratch model exhibited consistent improvements in validation accuracy throughout training (see Fig. 3a), reflecting steady feature acquisition. In contrast, the fine-tuned model showed less monotonic progression with multiple local maxima and minima in validation performance (see Fig. 3b). The fine-tuned pattern emerged from the need of adapting to new task requirements while overcoming previously learned representations that may no longer be relevant. The convergence of both models suggests that while fine-tuning requires more iterations to reconcile these competing objectives, both approaches ultimately reach comparable stability.

E. Evaluation Metrics

The performance of the proposed models was evaluated using standard classification metrics, including accuracy, precision, recall, and F1-score. Each metric provided different insights into the model's effectiveness, with specific clinical implications. Sensitivity is particularly important in medical applications where false negatives must be minimized [10], as missing a BrS case could lead to severe consequences, including an undiagnosed risk of sudden cardiac arrest.

IV. Results and Discussion

A. Binary Adaptation to Ternary Classification

The threshold-adapted binary model produced distinct probability distributions: Non-BrS (0.12 ± 0.21), Definitive (0.97 ± 0.04), and Borderline (0.85 ± 0.20). The Borderline class showed particularly high variability, with many probabilities nearing the Definitive threshold, revealing inherent limitations of binary classification for intermediate ECG morphologies. These findings strongly support developing a dedicated three-class classifier for more stable predictions.

1) Fine-Tuned Model Performance: As shown in Table IV, the fine-tuned model reached *Precision* and *Recall* values of 0.77 and 0.88 for the Definitive class, alongside 0.85 and 0.80 for the Borderline class. Figure 4a reveals that most Definitive Brugada instances were correctly recognized, but several Borderline cases were incorrectly labeled as Definitive or vice versa. While maintaining good sensitivity for the Definitive category, the fine-tuned approach showed a slightly lower overall accuracy (0.88), partly due to misclassifications in the Borderline class.

2) From-Scratch Model Performance: In contrast, Table V indicates that the from-scratch model obtained higher performance across all three classes, with 0.98 precision and 1.00 recall for Non-BrS, and approximately 0.92 F1-scores for both Definitive and Borderline. As illustrated in Figure 4b, the model exhibited fewer overall misclassifications, leading to a final accuracy of 0.94. Notably, the perfect recall for Non-BrS indicated minimal false positives in that class, reducing unnecessary follow-up for healthy individuals.

3) Direct Comparison on the Two Test Sets Intersection: Both models were evaluated on an identical subset of 74 test samples (42 Non-BrS, 18 Borderline, 14 Definitive) to control for dataset imbalances. Despite the limited sample size, the from-scratch model showed superior performance (96% vs 92% accuracy), particularly for minority classes: Definitive achieved a 0.96 F1-score (vs 0.84) with perfect precision (1.00) and 0.93 recall, while Borderline reached 0.91 F1-score (vs 0.82) through improved recall (0.89 vs 0.78). Both models excelled on Non-BrS cases (F1 $\geq$ 0.98). Though constrained by sample size, these results indicate the from-scratch approach more effectively identifies subtle features in challenging BrS cases.

The difference in performance has direct clinical relevance. Failing to detect an actual Brugada ECG (*false negative*) poses significant risks for patient safety. Conversely, overdiagnosing a Non-BrS case as Brugada could lead to unnecessary testing.

The from-scratch model's higher accuracy and balanced metrics make it well-suited for settings where minimizing both false negatives and false positives is paramount. However, its training process requires more data. Meanwhile, the fine-tuned model—despite slightly lower overall accuracy—could still be advantageous if domain-specific knowledge is incorporated or if dataset size is limited.

B. Error Analysis and Misclassification Patterns

1) Lead-Level Analysis (Aggregated Prediction per Lead): The error analysis in Table VI refers to the classification of entire ECG leads rather than individual 850 ms windows, which are the true inputs to the network. Since each lead is composed of multiple QRST windows, the errors reported here correspond to the number of misclassified leads, not individual windows.

The total misclassifications decreased from 55 to 26 after fine-tuning, indicating better overall robustness. Notably, *Non-*

TABLE IV
TEST SET PERFORMANCE OF THE FINE-TUNED MODEL.

Class	Precision	Recall	F1-Score
Non-BrS (0)	0.97	0.94	0.96
Definitive (1)	0.77	0.88	0.82
Borderline (2)	0.85	0.80	0.82
Accuracy		0.88	
Macro Avg	0.86	0.87	0.87
Weighted Avg	0.88	0.88	0.88
Total Samples		534	

TABLE V
TEST SET PERFORMANCE OF THE FROM-SCRATCH MODEL.

Class	Precision	Recall	F1-Score
Non-BrS (0)	0.98	1.00	0.99
Definitive (1)	0.91	0.92	0.92
Borderline (2)	0.92	0.88	0.90
Accuracy		0.94	
Macro Avg	0.94	0.93	0.93
Weighted Avg	0.94	0.94	0.94
Total Samples		518	

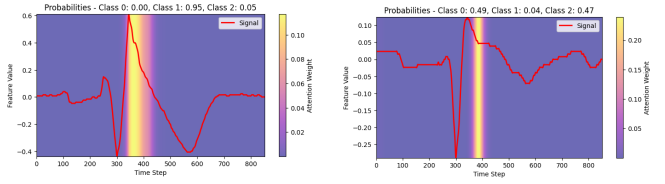
Brugada leads misclassified as Borderline dropped from 28 to 5, suggesting improved differentiation of normal ECGs from those with Brugada-like features. However, *Non-Brugada leads misclassified as Definitive* rose from 1 to 10, due in part to the attention mechanism focusing on regions morphologically similar to the Brugada ST segment. Although this leads to slight overdiagnosis, it remains preferable to false negatives in clinical practice. The number of *Borderline leads misclassified as Definitive* decreased from 20 to 4, reducing the risk of labeling uncertain cases as definite BrS. Conversely, *Definitive leads misclassified as Borderline* increased from 1 to 3, indicating a more conservative approach to borderline presentations. Finally, there were no Definitive leads misclassified as Non-Brugada in either model, and Borderline-to-Non-Brugada errors slightly decreased, all pointing to improved specificity.

These observations suggest that while the fine-tuned model achieved higher specificity and maintained very low false negatives, some improvements would help to guide the attention mechanism away from Brugada-like morphologies that appear in non-diagnostic regions of the ECG.

2) Error Interpretability Through Attention Maps: To further investigate these misclassifications, Figure 5 shows attention heatmaps highlighting the regions that drove each prediction. In Figure 5a, the fine-tuned model focus aligned well with the segment clinically recognized as critical for Brugada pattern identification, leading to a correct prediction. Figure 5b instead illustrates a case where the model trained from scratch struggled to distinguish Non-Brugada from Borderline: the attention map clarifies the diagnosis since it specifically highlights the ST segment portion with isoelectric line hesitation, which is a hallmark pattern seen in RBBB or NIVCD that resemble Brugada pattern (see Fig. 2). This

TABLE VI
COMPARISON OF ERROR TYPES BETWEEN THE ADAPTED BINARY MODEL AND THE FINE-TUNED MODEL ON THE SAME TEST SET.

Error Type (GT to pred)	Binary Adaptation	Fine-Tuned
Non-BrS to Definitive	1	10
Non-BrS to Borderline	28	5
Definitive to Non-BrS	0	0
Definitive to Borderline	1	3
Borderline to Non-BrS	5	4
Borderline to Definitive	20	4
Total	**55**	**26**



(a) (b)

Fig. 5. Attention maps highlighting different model behaviors: (left) correctly classified *Definitive* Brugada pattern window by the fine-tuned model; (right) test window where the model trained from scratch shows uncertainty between *Non-Brs* and *Borderline*.

precise localization of electrophysiological anomalies shows the model's clinically meaningful decision-making pattern.

C. Distribution of ECG Lead-Level Predicted Probabilities

Figure 6 illustrates the distribution of predicted probabilities by the fine-tuned model for each ground truth class, computed as the average of all the 850 ms window-level probabilities within a lead. This representation highlights how the fine-tuned model behaved when applied to an entire ECG derivation, which is the closest approach to real-world clinical assessment.

The results confirmed that the model was able to effectively discriminate the three classes at the lead level. Non-BrS leads exhibited high classification confidence, with an average predicted probability of approximately 0.90 assigned to the correct class. This suggested that the model had learned to reliably recognize non-pathological patterns with minimal ambiguity.

For the Definitive class, the model assigned the highest probability to the correct category (0.67 on average), but a non-negligible proportion of predictions were distributed toward the Borderline class (0.32). A similar effect was observed for Borderline leads, which received the highest probability in their own class (0.68) but also showed partial overlap with Definitive predictions (0.16). This phenomenon was expected given the nature of BrS: in clinical settings, patients with Brugada can exhibit both definitive diagnostic (Type 1) and borderline samples within the same lead. Consequently, the model's probabilistic output reflected this physiological variability rather than representing a classification failure.

Overall, this distribution supports the idea that a lead-level classification approach, aggregating QRST-wise predictions,

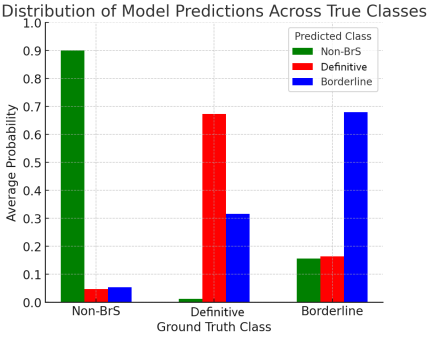


Fig. 6. Distribution of predicted probabilities for each ground truth class. The x-axis represents the true class labels, while the y-axis shows the average predicted probabilities for each class.

allows for a clinically meaningful distinction between the three categories. These findings suggest that probabilistic outputs could be useful in guiding clinical decision-making, potentially complementing existing diagnostic criteria.

V. Challenges and Future Developments

Despite the strong performance of the proposed model, key challenges remain. A primary limitation is the dataset size, particularly the scarcity of ECGs from Brugada patients with documented arrhythmic events. A larger, more diverse dataset could improve generalization and robustness, reducing potential biases.

Beyond classification, refining risk stratification is crucial. It remains unclear how the likelihood of arrhythmic events correlates with different ECG manifestations of BrS, particularly between Definitive and Borderline Type 1 patterns. Incorporating clinical data—such as genetic markers or pharmacological test outcomes—could enhance the model's predictive value.

Interpretability also requires improvement. While attention maps highlight key ECG regions, the model does not always focus exclusively on the ST segment, as clinically expected. A possible enhancement could involve modifying the loss function to penalize attention outside this region, aligning model predictions with clinical knowledge. However, this trade-off between accuracy and the model's ability to detect unexpected patterns requires careful evaluation.

Despite the promising results, to the best of author knowledge, this study represents the first publicly available approach to handle doubtful cases as a separate third class in BrS diagnosis. Future work will focus on benchmarking the model against other DL approaches, e.g. binary classifiers, and classical rule-based ECG systems, while expanding the dataset, improving risk prediction, and refining model constraints for greater clinical alignment. With continued development, AI-driven ECG analysis could become a valuable tool for both Brugada diagnosis and personalized risk assessment.

References

[1] J. Brugada, R. Brugada, and P. Brugada, "Right bundle-branch block and st-segment elevation in leads v1 through v3: a marker for sudden death in patients without demonstrable structural heart disease," *Circulation*, vol. 97, no. 5, pp. 457–460, 1998.

[2] J. Brugada, O. Campuzano, E. Arbelo, G. Sarquella-Brugada, and R. Brugada, "Present status of brugada syndrome: Jacc state-of-the-art review," *Journal of the American College of Cardiology*, vol. 72, no. 9, pp. 1046–1059, 2018.

[3] A. A. Wilde, C. Antzelevitch, M. Borggrefe, J. Brugada, R. Brugada, P. Brugada, *et al.*, "Proposed diagnostic criteria for the brugada syndrome: consensus report," *Circulation*, vol. 106, no. 19, pp. 2514–2519, 2002.

[4] P.-A. Călburean, L. Pannone, C. Monaco, D. D. Rocca, A. Sorgente, A. Almorad, *et al.*, "Predicting and recognizing drug-induced type i brugada pattern using ecg-based deep learning," *Journal of the American Heart Association*, vol. 13, no. 10, p. e033148, 2024.

[5] S. Liao, M. Bokhari, P. Chakraborty, A. Suszko, G. Jones, D. Spears, *et al.*, "Use of wearable technology and deep learning to improve the diagnosis of brugada syndrome," *Clinical Electrophysiology*, vol. 8, no. 8, pp. 1010–1020, 2022.

[6] C.-M. Liu, C.-L. Liu, K.-W. Hu, V. S. Tseng, S.-L. Chang, Y.-J. Lin, *et al.*, "A deep learning–enabled electrocardiogram model for the identification of a rare inherited arrhythmia: Brugada syndrome," *Canadian Journal of Cardiology*, vol. 38, no. 2, pp. 152–159, 2022.

[7] E. Pasero, F. Gaita, V. Randazzo, P. Meynet, S. Cannata, P. Maury, *et al.*, "Artificial intelligence ecg analysis in patients with short qt syndrome to predict life-threatening arrhythmic events," *Sensors*, vol. 23, no. 21, p. 8900, 2023.

[8] V. Randazzo, G. Marchetti, C. Giustetto, E. Gugliermina, R. Kumar, G. Cirrincione, *et al.*, "Learning-based approach to predict fatal events in brugada syndrome," in *Applications of Artificial Intelligence and Neural Systems to Data Science*, pp. 63–72, Springer, 2023.

[9] S. Caligari, V. Randazzo, F. Gaita, C. Giustetto, M. Millesimo, and E. Pasero, "A neural network approach for the prediction of arrhythmic events in patients with brugada syndrome via ecg features analysis," in *2024 IEEE 22nd Mediterranean Electrotechnical Conference (MELECON)*, pp. 329–333, IEEE, 2024.

[10] V. Randazzo, S. Caligari, E. Pasero, C. Giustetto, A. Saglietto, W. Bertarello, *et al.*, "A vision transformer model for the prediction of fatal arrhythmic events in patients with brugada syndrome," *Sensors*, vol. 25, no. 3, p. 824, 2025.

[11] F. Gaita, N. Cerrato, A. Saglietto, D. Caponi, L. Calò, and C. Giustetto, "The brugada syndrome: risk stratification," *European Heart Journal Supplements*, vol. 25, no. Supplement_C, pp. C27–C31, 2023.

[12] P. Rattanawong, J. Kewcharoen, C. Kanitsoraphan, W. Vutthikraivit, P. Putthapiban, N. Prasitlumkum, *et al.*, "The utility of drug challenge testing in brugada syndrome: A systematic review and meta-analysis," *Journal of cardiovascular electrophysiology*, vol. 31, no. 9, pp. 2474–2483, 2020.

[13] C. Pappone and V. Santinelli, "Brugada syndrome: progress in diagnosis and management," *Arrhythmia & electrophysiology review*, vol. 8, no. 1, p. 13, 2019.

[14] M. J. Cutler, L. L. Eckhardt, E. S. Kaufman, E. Arbelo, E. R. Behr, P. Brugada, *et al.*, "Clinical management of brugada syndrome: commentary from the experts," *Circulation: Arrhythmia and Electrophysiology*, vol. 17, no. 1, p. e012072, 2024.

[15] H. Morita, K. F. Kusano, D. Miura, S. Nagase, K. Nakamura, S. T. Morita, *et al.*, "Fragmented qrs as a marker of conduction abnormality and a predictor of prognosis of brugada syndrome," *Circulation*, vol. 118, no. 17, pp. 1697–1704, 2008.

[16] G. Zahn, J. L. Welch, and S. Roumpf, "Distinguishing between brugada and incomplete right bundle branch block on ecg," *Visual Journal of Emergency Medicine*, vol. 16, 2019.

[17] S. Caligari, V. Randazzo, C. Giustetto, F. Gaita, and E. Pasero, "Predictive recognition of brugada syndrome patterns in digital signal data using neural networks," *Neural Networks: Overview of Current Theories and Applications*, in press.

[18] GE HealthCare, "Ge healthcare italia." https://www.gehealthcare.it.

[19] Powerful Medical, "Pmcardio by powerful medical." https://www.powerfulmedical.com/pmcardio.

[20] J. Enders, W. Geng, P. Li, M. W. Frazier, and D. J. Scholl, "The shift-invariant discrete wavelet transform and application to speech waveform analysis," *The Journal of the Acoustical Society of America*, vol. 117, no. 4, pp. 2122–2133, 2005.

[21] D. Bahdanau, K. Cho, and Y. Bengio, "Neural machine translation by jointly learning to align and translate," *arXiv preprint arXiv:1409.0473*, 2014.